

Orientation Estimation for Multiple Large Fractures by Scattering Energy

Yang Zhang, Shihong Chi, Mark E. Willis, M. Nafi Toksöz, and Dan Burns

Earth Resources Laboratory
Dept. of Earth, Atmospheric and Planetary Sciences
Massachusetts Institute of Technology
Cambridge, MA 02139

Abstract

We have done the numerical modeling of seismic response to multiple sets of vertical large fractures by using finite-difference method (FD), which can easily handle media with monoclinic anisotropy. We consider three types of fracture distributions: a set of parallel fractures, two sets of orthogonal fractures and two sets of non-orthogonal fractures intersecting at 45 degrees. We address the seismic scattering response to large fractures by using a 3-layer model and a 5-layer model, where a fractured reservoir is in the middle layer of these two models. Seismic scattered energy is analyzed by the Scattering Index (SI) method to estimate the orientation of these multiple fractures. In both models, SI indicates the correct orientation of the two orthogonal fracture sets but is ambiguous for non-orthogonal fracture sets. Information about the fracture spacing and compliance can also be extracted from the azimuthal SI in some situations. More compliant fracture sets result in higher SI values while the relationship between fracture spacing and SI depends on the source wavelength. Variations in the SI energy can be caused by fracture spacing and compliance variations, and these relationships need further investigation.

1. Introduction

With increasing interest in carbonate and unconventional (e.g., tight gas) reservoirs, fracture characterization has become an important research topic. When the seismic wavelength is much larger than the scale of the cracks or fractures in length and spacing, effective media theories can be used to describe the seismic response to fractures in the reservoir (e.g., Hudson, 1980, 1981; Schoenberg et al., 1980, 1988, 1995, 1997; Kachanov, 1980, 1992, 1993). Due to natural stress fields, the fractures in a reservoir usually are vertical or sub-vertical and have a preferred orientation parallel to the maximum horizontal stress direction, which could induce the seismic anisotropy. When a seismic wave propagates through an anisotropic medium the P wave shows an AVOAz (amplitude variation with offset and azimuth) response, an elliptical NMO velocity response with azimuth, and shear wave splitting. To take advantage of these seismic signatures, effective media theories provide the mathematical framework which has been used for inversion processes to get the parameters related to the fractured reservoir, such as fracture orientation, crack density and even properties of the fracture fill material.

However, cracks or fractures seldom distribute evenly in the subsurface as assumed in effective media theories. Often fractures will cluster onto large scale fracture corridors or zones, which can have much more impact on production. Recent research shows that the seismic response to such large fracture zones is quite different from that described by effective media theories. The response depends on fracture size, spacing, and distribution (Vlastos, et al., 2003; Chi, et al., 2006). Since the scale of fractures in such settings is comparable to the seismic wavelength, the prominent characteristic of seismic response is seismic scattering, which includes energy diffracted from fractures and reverberating within fracture zones. The strong scattered energy can make it difficult to identify coherent events in the seismic section (Willis, et al., 2006; Chi, et al., 2006). Zhang et al. (2005) numerically studied the AVOAz responses of PP reflections from the top of a reservoir containing large scale discrete fractures, and compared them to the responses obtained from reservoirs containing small cracks (i.e., effective media representation). They showed that in the case with large discrete fractures, the AVOAz for the PP reflections from the top of the reservoir had noticeable differences in magnitude and phase from those of the effective media case. Willis et al. (2006) studied the features of seismic scattering from one set of aligned discrete fractures, and estimated the orientation of the fractures by analyzing the scattered energy at different azimuths. Also

Willis et al. (2005) used the spectral notches of the scattered energy to estimate the fracture spacing. Grandi et al. (2005) and Zhang et al. (2006) estimated the fracture spacing by FK analysis of the backscattered energy from discrete fracture zones from P to P and P to S scattered energy.

These previous studies suggest that scattered energy from discrete fracture zones can be useful for fracture characterization, however most have focused on one set of aligned fractures. It is more likely that multiple sets of fractures are present in field settings, even if one set is more dominant due to the in-situ stress field. Much effort has been spent in considering the effect of multiple fracture sets in effective media theories (e.g., Nichols, et al., 1989; Grechka, et al., 2003; Grechka and Kachanov, 2006). A promising conclusion drawn by Grechka and Kachanov (2006) is that no matter how many vertical small cracks there are and how they orient and what types of infill they contain, the effective medium can be approximately described as orthorhombic. Geological observation suggests that there could be two or more sets, depending on the geological history in that particular area, of conjugate fractures coexisting. These sets of large fractures can be orthogonal or non-orthogonal to each other. For vertical large fracture sets in one fixed Cartesian coordinate system, such sets would give rise to media with different anisotropic symmetry, such as HTI, orthorhombic and monoclinic.

Chi et al. (2006) carried out a numerical study of the seismic scattering from multiple sets of vertical large fractures by using the finite difference method. They carefully handled these anisotropic media by assigning different effective elastic constants to the grid cells where fractures or the intersection of fractures were located. The effective constants for the fracture grid cells were calculated by the method developed by Coates and Schoenberg (1995). A simple 3-layer model with a fractured reservoir in the middle layer was used to emphasize on the scattering patterns due to multiple fracture sets. By analyzing the forward modeling results from different configurations of fractures sets, they addressed qualitatively the relationship between the patterns of scattered energy and the orientations, elastic properties, and spacing of the fracture sets. We might note that Willis et al (2004) had considered the case with dual fracture sets but simplified the fracture properties by using homogeneous and isotropic media directly. As mentioned earlier, Willis et al (2006) developed a method, called the Scattering Index (SI), to extract the orientation information of one single set of aligned fractures from variations in the scattered energy as a function of azimuth. The question we want to answer in this paper is whether the SI method can work on cases with multiple sets of fractures, and further to discuss whether the transfer function or the stacked traces can give us some new information about such multiple fracture sets.

This paper is organized in four sections: 1) a brief review of the numerical modeling work done by Chi et al (2006), since we will use their data for our SI analyses; 2) the analysis of the 3-layer model data by the SI method; 3) the analysis of one 5-layer model with multiple fracture sets; and 4) a discussion of the results.

2. Numerical Modeling of Multiple Sets of Fractures

Although the length and spacing of large fracture zones are comparable to the seismic wavelength, they are composed of many cracks that may contain weaker material such as oil, water and gas. These infill materials cause the fracture zones to be much more compliant than the background matrix material. As a result, fractures can behave mechanically as discontinuous interfaces, through which seismic wave induced displacements are discontinuous while tractions are continuous (Schoenberg, 1980). Schoenberg and Sayers (1995) mathematically derived a linear slip relationship to link the displacements and tractions with a factor Z , the fracture compliance, which describes the mechanical properties of fractures. Schoenberg and Sayers (1995) showed that the effective properties of media containing multiple fracture sets can be gotten by adding each set of fractures sequentially. Chi et al (2006) used a similar procedure, treating the finite difference cells containing intersecting fractures as multiple sets of fractures, while all other cells contained either a single fracture or the background material. In this paper, we only consider vertical fractures and a maximum of two fracture sets.

For a given coordinate system, the anisotropy for a single fracture set aligned with the coordinate axes would be HTI (horizontal transverse isotropy), and for a single fracture set oriented at an angle to the

axes the anisotropy would be monoclinic. For two sets of orthogonal fractures, the material at the intersection would be orthorhombic, and for those of non-orthogonal intersecting fractures, monoclinic it would be (Chi et al., 2006). Coates and Schoenberg (1995) introduced a method to represent the fractures in finite difference grids by calculating the effective constants for grid cells where fractures intersect. Once we get these effective constants, we can assign them onto grid cells corresponding to the locations of fractures. Figure 1 shows three types of fracture models considered in this paper: one set of aligned fractures, two orthogonal fracture sets and two non-orthogonal fracture sets intersecting at 45 degrees. Different colors represent materials with different anisotropic properties.

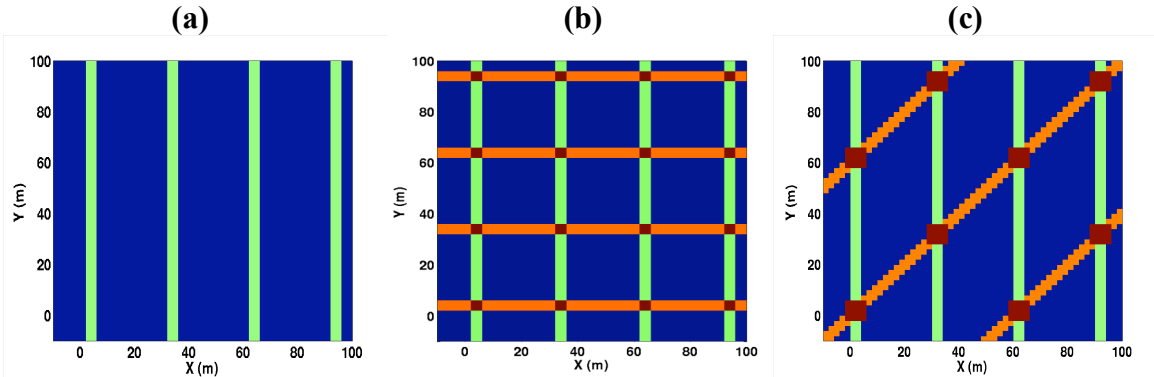


Figure 1: Three fracture models: (a) one set of aligned fractures; (b) two orthogonal fracture sets; (c) two non-orthogonal fracture sets intersecting at 45 degrees.

3. Orientation Estimation for Multiple Sets of Fractures with SI Method

The Scattering Index (SI) method developed by Willis et al. (2006) is a technique to estimate the orientation of aligned large fractures by capturing the azimuthal variation of the coherence of seismic scattering energy from fracture zones. The method was derived from numerical data analysis and has been successfully applied to onshore and offshore field data from fractured carbonate reservoirs. However, the methodology was developed with the assumption of a single set of aligned fractures and it is not clear if the method will work if there are multiple fracture sets present. Chi et al (2006) showed that the scattered wavefield generated from multiple sets of fractures is much more complicated than that of a single set of fractures, adding to this concern. To answer this question, we generate numerical waveforms for a 3 layered and 5 layered model. The middle layer in each contains fractures with one of the three types of fracture distributions shown in Figure 1. Figure 2 shows the model configuration for 3-layer model, in which source and receivers are at the surface, and the acquisition azimuths have been defined.

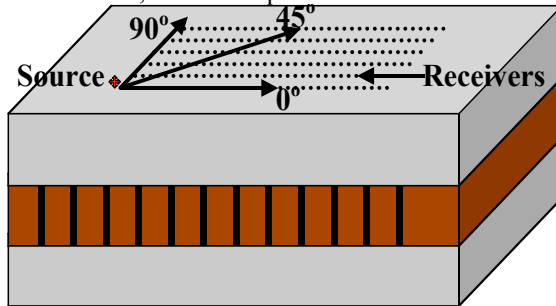


Figure 2: A three-layered model for fractured reservoir.

4. Results and Discussion

4.1 Model with 3 Layers

For this case, as shown in Figure 2, one fractured layer is embedded within two homogenous, isotropic layers. Large fractures in this layer are distributed in form of each of the models shown in Figure 1. The spacing for fracture set aligning at 90 degrees is set to 30 m (Figure 1a), denoted as **X30**, while the spacing for the one orthogonally aligned is set to 30 m (**X30** \perp **Y30**) and 42 m (**X30** \perp **Y42**) respectively as shown in Figure 1b. For non-orthogonal fracture sets, the fractures oriented at 45 degrees have a spacing of $30 \cdot \sqrt{2} \approx 42$ m (**X30** \angle **45**), as shown in Figure 1c. The fractures we consider are rotationally invariant with normal and transverse compliance being equal. For most cases considered here, we choose fracture compliances $Z_N = Z_T = 2 \times 10^{-10}$ m/Pa for all fracture sets. For the case of **X30** \perp **Y30** we also investigate unequal compliance for different fracture sets. We set the compliance value for the fracture set aligned at 0 degree (**Y30**) to be four (4) times large than the fractures at 90 degrees (**X30**). This situation is denoted as **X30** \perp **Y30Z4** \times . One case without fractures (**NoFrac**) is used as a reference (Figure 3a). For More details about the numerical modeling, please refer to the work by Chi et al. (2006).

For models without fractures and with parallel and orthogonal fractures, we sort the common-shot gathers in azimuths from 0 to 90 degrees at an increment of 10 degrees. A gather at an azimuth 45 degrees is also included. Especially for multiple non-orthogonal fracture sets intersecting in 45 degrees to each other, the range of azimuth should vary from 0 to 180 degrees because of the lower symmetry of the model configuration. Following the method of Willis et al (2006), we first use the shot gathers of the **NoFrac** model to do a velocity analysis and obtain the NMO velocities of the PP events at each azimuth (which should be equal theoretically). We then apply these NMO velocities on the azimuthal shot gathers for the rest models. We stack the traces of these NMOed shot gathers at offsets within 400 m. Figure 3a shows the stacked traces in azimuth for the model without fractures. Two strong events at times of about 550 ms and 650 ms represent the reflected PP wave from the top and bottom of the reservoir. The amplitudes of these arrivals have no azimuthal variation and no scattering energy arrives at later times. For using the SI method on the models containing fractures, we pick two time windows, the input and output windows, which are indicated by red and blue boxes respectively in Figure 3a. The longer output window is chosen to capture most of the scattering energy due to large fractures in the other models.

Applying the NMO velocities for the model without fractures on the data for models with fractures we get the stacked traces shown in Figure 3b to 3f. The most significant phenomenon for these traces is the coda energy existing at later times due to the scattering from the large fractures. For models with only one set of parallel fractures (Figure 3b), strong scattered energy is seen at the azimuth of 90 degrees, which is parallel to the fractures. After stacking, coherent scattered energy gets strong, while incoherent energy (that is, the combination of forward and back scattering) gets cancelled out. The result is that scattered energy stacks in at the azimuth that is parallel to the fracture direction. Due to symmetry of the configuration, the model with two sets of orthogonal fractures with equal compliances and spacing gives equally strong scattered energy at 0 and 90 degree azimuths, which are parallel to each set of fracture respectively (Figure 3c). Relatively small scattered energy is seen in the middle range of azimuths. For models with one set of more compliant fractures (Figure 3d), we see that the PP reflection from the bottom of the reservoir is mostly contaminated by the scattered wave energy. Strong scattered energy shows at all azimuths, and the scattered energy at 0 degrees is stronger than that at 90 degrees. This suggests that the more compliant fracture set contributes much more to the scattered wavefield. For models with two sets of fractures but with different spacing (Figure 3e), the azimuthal variation of scattered energy is somewhat similar to that for one set of parallel fractures (Figure 3b) except that a small amount of scattering is also seen at 0 degree azimuth, which is due to the second fracture set with larger spacing. Comparing energy in Figure 3d and 3e, we see that spacing and compliance both have an effect on stacked energy, but the compliance factor has the larger effect. The final model has two sets of non-orthogonal fractures at 45 degrees to one another. Figures 4f shows that the scattered energy varies azimuthally from 0 to 180 degrees. The strongest scattered

energy is seen at 90 degrees, which is parallel to the fracture set with 30 m spacing. There is a small amount of scattered energy visible at 45 degrees arriving at 900 ms.

To compute the SI attribute we can apply the input and output time windows to the azimuthal stacks in Figure 3 to isolate the signals for the deconvolutional process, which at the end gives us the transfer function linking these two signals (Willis et al., 2006). Being like a filter, the fractured reservoir takes in the simple input signal and converts it into the more complicated output signal. The transfer function describing the filter characterizes the degree of scattering due to the discrete large fractures in the reservoir. By calculating the L1-norm of the transfer function, Willis et al (2006) derived a quantity, scattering index (SI), as a seismic attribute of scattering to determine the orientation of fractures.

Figure 4 shows the scattering index (SI) values as a function of azimuth for cases with and without fractures. The SI values are calculated for azimuths between 0 and 90 degrees, and these values are then projected into the other quadrants based on symmetry. For the model without fractures there is no scattered energy and the SI values show no azimuthal variation (Figure 4a). For the model with one set of aligned fractures (Figure 4b), there is a large SI amplitude at an azimuth of 90 degrees, which is the orientation direction of the fracture set. Figure 4c shows the SI values for the model with two sets of orthogonal fractures having equal fracture spacing. High amplitudes are seen at azimuths of 0 and 90 degrees, indicating the orientation of the two sets of fractures respectively. This result, where the two fracture sets have the same compliance, can be compared to the case where the fracture compliance values are different. Figure 4d shows the results for the same two sets of orthogonal fractures as shown in Figure 4c, however in this case the fracture set oriented at 0 degrees has a compliance that is four times larger than the set oriented at 90 degrees. In the direction parallel to the more compliant set of fractures (0 degrees) the SI amplitude is about four times larger than the amplitude at 90 degrees, which is parallel to the less compliant fracture set. This is an encouraging result that suggests the possibility of using the scattered energy amplitude as a measure of fracture compliance, which could be related to fracture aperture and therefore permeability. However, such an approach must be entered into cautiously because of the ambiguity between fracture spacing and compliance. Figure 4e illustrates this point. For a model with two sets of orthogonal fractures but having unequal spacing, we see a pattern in the SI values that is similar to that seen with different compliance values. In this situation the highest SI amplitudes are in the direction parallel to the smaller fracture spacing (90 degree orientation, 30 m spacing), with a much smaller SI value peak (about a factor of three smaller) in the direction of the fracture set with larger spacing (0 degrees, 42 m spacing). The relationship between scattered wave energy and fracture spacing will be a function of the seismic wavelength. Because of the similar response of the SI attribute to changes in fracture compliance and spacing, it is important to find ways to differentiate between these two effects. Zhang et al. (2006) and Willis et al. (2006) have used the backscattered energy and spectral notches respectively to estimate the fracture spacing from the scattered wave energy. Such approaches might provide us with a means of separating the effects of spacing and compliance and allow us to isolate the effect of fracture compliance. The final model is for two sets of non-orthogonal fractures, one set oriented at 90 degrees and the second set oriented at 45 degrees. Both fracture sets have the same compliance, but the spacing is different (larger spacing for the fracture set at 45 degrees). In this case we need to investigate the scattering in the azimuth range from 0 to 180 degrees in order to cover fully the scattering for both fracture sets. The resulting SI values are plotted from 0 to 180 degrees, which is symmetric for the 180 to 360 degree azimuths. Figure 4f shows that the SI values are largest at 90 degrees, the orientation of one set of fractures (with the smaller spacing), while the other azimuths show much smaller values. We can infer that another set of fracture is present, which could be oriented at 30, 45, or 135 degrees based on the SI distribution (which is clearly different from that seen for a single set of fractures as in Figure 5b). For this simple 3-layer model, the stacked traces in Figure 3f would suggest that the second fracture set is at 45 degrees, however the SI values are less clear.

4.2 Model with 5 layers

In the three layer model, it is quite easy to pick out the reflections from the top and base of the reservoir, even in the presence of significant scattering. However, in actual field situations there will be many reflectors present and it will not be easy to isolate these reflectors for SI analysis. In order to test the methodology in a slightly more realistic situation we generate a second set of models containing 5 layers.

In these models we will use a larger sampling window containing several reflected events for the SI analysis, as was shown by Willis et al. (2006). The ‘input’ wavelet is estimated from a window containing reflection events above the reservoir level, and the ‘output’ wavelet is estimated from a window containing reflection events below the reservoir level. The transfer function is estimated from these wavelets via a deconvolutional process.

Choosing the same parameters for the background media and fracture compliance used by Willis et al. (2006), we modeled the seismic response to discrete large fractures embedded in the middle layer. The same three types of fracture model shown in Figure 1 are considered, but for these models the fracture spacing is set at 35 m to provide maximum scattering for this set of parameters (Willis et al., 2006). In this case the spacing between fractures orientated at 45 degrees is about 50 m, so there are a total of six cases considered in this section: **NoFrac**, **X35**, **X35 \perp Y35**, **X35 \perp Y35Z4 \times** , **X35 \perp Y50** and **X35 \angle 45**.

Figure 5a shows the azimuthal stacked traces for the model without fractures. Four arrivals are seen, which correspond to the PP reflected waves at each interface in the model. We take a window (red) including first two reflected PP events as the input signal, and then another window (blue) including the last two as the output signal. These two time windows will be applied on the azimuthal stacked traces for the other models as well.

Azimuthal stacked traces for all the different models are shown in Figure 5 and most of the same trends seen for the 3-layer models are present. For the model with a single set of parallel fractures (Figure 5b), strong scattered energy remains after stacking in the direction parallel to the fracture strike. For the model with two sets of orthogonal fractures with the same spacing (Figure 5c) strong energy is seen in the two directions parallel to the two sets of fractures. When one fracture set is four times more compliant, the more compliant fracture set induces stronger scattered energy in the direction parallel to its strike (Figure 5d), although the difference in amplitude is not as great as it was in the 3-layer model (Figure 3d). Figure 5e shows the results for a model with two sets of orthogonal fractures but with different spacing. For the 3-layer model we observed that the fracture set with smaller spacing (30 m) induced stronger scattered energy than the one with larger spacing (42 m). However for the 5-layer model, the fracture set with the larger spacing (50 m) seems to give slightly stronger energy than smaller spacing does (35 m), although the difference is quite small. This may be due to somewhat different source wavelengths in the two models. The final model is for two sets of non-orthogonal fractures, oriented at 90 and 45 degrees (Figure 5f). We still see strong scattered energy in the 90 degree direction along with significant scattered energy at most other azimuths although higher amplitudes are seen around 45 degrees, the orientation of the second set of fractures.

Applying the time windows defined in Figure 5a to each set of model azimuthal stacks we compute the SI values, which are shown in Figure 6. For the model without fractures (Figure 6a), the SI values are small and approximately equal at all azimuths. For one single set of parallel fractures, the SI value is a maximum in the direction of the fracture strike (Figure 6b). The three cases with orthogonal fracture sets are shown in Figures 6c, d and e respectively. All of them give a clear indication of the orientations for both sets of fractures. We notice that the SI plots in Figures 6d and 6e look similar, with the maximum SI value being at 0 degrees. In Figure 6d this direction corresponds to the fracture set with largest compliance, while in Figure 6e this direction corresponds to the fracture set with the larger spacing, which shows again the ambiguity between compliance and spacing. In Figure 6f, the SI peak is at 90 degrees indicating the set of fracture with 35 m spacing with a broad area of increase SI values around is at 30 to 50 degrees.

Acknowledgements

This work was supported by the Founding Member Consortium at the Earth Resources Lab, and DOE Award No. DE-FC26-02NT15346.

References:

- Chi, S. H., Zhang, Y., Campman, X. and Toksöz, M. N., 2006 Finite difference modeling seismic responses to intersecting fractures, 2006 ERL Consortium Meeting Report
- Coates, R. T. and Schoenberg, M., 1995, Finite-difference modeling of faults and fractures, *Geophysics*, 60, 5, 1514-1526
- Grandi, S., Willis, M. E., Burns, D. R. and Toksöz, M. N., 2005, F-K analysis of backscattered signal to estimate fracture orientation and spacing, 2005 ERL Consortium Meeting Report
- Grechka, V. and Tsvankin, I., 2003, Feasibility of seismic characterization of multiple fracture sets, *Geophysics*, 68, 1399-1407
- Grechka, V. and Kachanov, M., 2006, Seismic characterization of multiple fracture sets: Does orthotropy suffice?, *Geophysics*, 71, ...
- Hudson, J. A., 1980, Overall properties of a cracked solid, *Math. Proc. Camb. Phil. Soc.*, 88, 371-384
- Hudson, J. A., 1981, Wavespeeds and attenuation of elastic waves in material containing cracks, *Geophys. J. Roy. Astr. Soc.*, 64, 133-150
- Kachanov, M., 1980, Continuum model of medium with cracks, *J. Eng. Mech. Div., ASCE*, 106, EM5, 1039-1051
- Kachanov, M., 1992, Effective elastic properties of cracked solids: Critical review of some basic concepts, *Appl. Mech. Rev.*, 45, 304-335
- Kachanov, M., 1993, Elastic solids with many cracks and related problems, *Adv. Appl. Mech.*, 30, 259-445
- Nichols, D., Muir, F., and Schoenberg, M., 1989, Elastic properties of rocks with multiple sets of fractures, *59th SEG Expanded Abstracts*, 471-474.
- Schoenberg, M., 1980, Elastic wave behavior across linear slip interfaces, *J. Acous. Soc. Am.*, 68, 1516-1521
- Schoenberg, M. and Douma, J., 1988, Elastic wave propagation in media with parallel fractures and aligned cracks, *Geophysical Prosp.*, 36, 571-590
- Schoenberg, M. and Sayers, C. M., 1995, Seismic anisotropy of fractured rock, *Geophysics*, 60, 1, 204-211
- Schoenberg, M., and Helbig, K., 1997, Orthorhombic media: modeling elastic wave behavior in a vertically fractured earth, *Geophysics*, 62(6), 1954-1974.
- Vlastos, S., Liu, E., Main, I. G. and Li, X. Y., 2003, Numerical simulation of wave propagation in media with discrete distributions of fractures: effects of fracture sizes and spatial distributions, *Geophysical J. International*, 152, 3, 649-668
- Willis, M., Rao, R., Burns, D. and Byun, J., 2004, Spatial orientation and distribution of reservoir fractures from scattered seismic energy, 2004 ERL Consortium Meeting Report.
- Willis, M., Rao, R., Burns, D. and Toksoz, M. N., 2005, Fracture spacing and orientation estimation from spectral analyses of azimuth stacks, Expanded abstract, EAGE meeting, Madrid.
- Willis, M., Burns, D. R., Rao, R., Minsley, B., Toksoz, M. N., Vetri, L., 2006, Spatial orientation and distribution of reservoir fractures from scattered seismic energy, *Geophysics*, in press.

Zhang, Y., Chi, S., Willis, M. E., Burns D. R. and Toksöz, M. N., 2005, Comparison of discrete fracture and effective media representation of fractures on azimuthal AVO, *75th SEG Expanded Abstracts*

Zhang, Y., Campman, X., Grandi, S., Chi, S. H., Willis, M. E., Toksöz, M. N. and Burns, D., 2006, Wavenumber-Frequency domain characteristics of the seismic response of a set of parallel discrete fractures, *76th SEG Expanded Abstracts* submitted

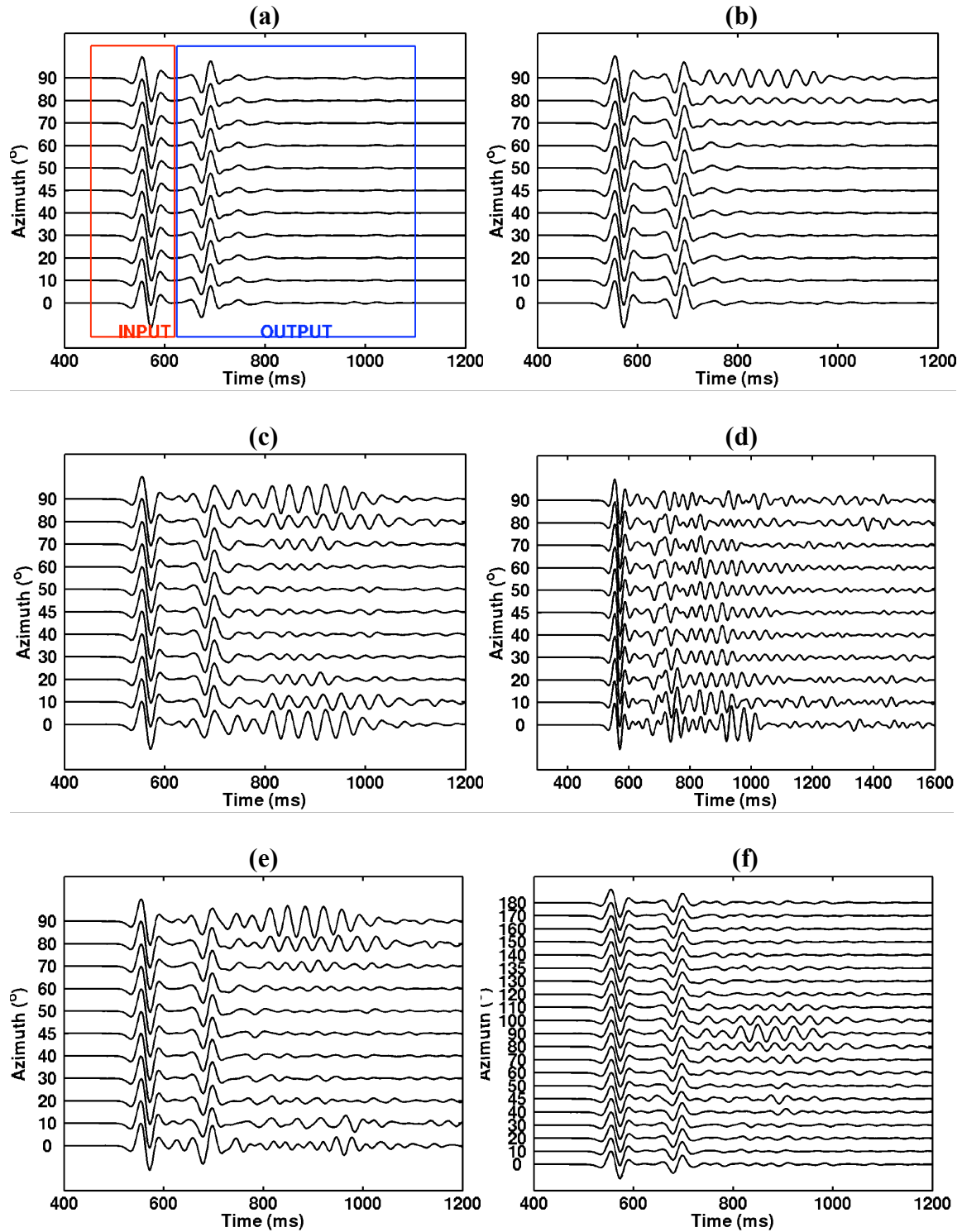


Figure 3: Azimuthal stacked traces for the 3-layer models. (a) no fractures; (b) single fracture set with a strike of 90 degrees (X_{30}); (c) two sets of orthogonal fractures with the same fracture compliance and spacing ($X_{30} \perp Y_{30}$); (d) same as (b) except compliance for fracture set aligned at 0 degrees is 4 times large than that at 90 degrees ($X_{30} \perp Y_{30Z4}$); (e) two sets of orthogonal fractures with different spacing ($X_{30} \perp Y_{42}$); (f) two sets of non-orthogonal fractures at 45 degrees, 0 to 180 degrees azimuth ($X_{30} \angle 45$);

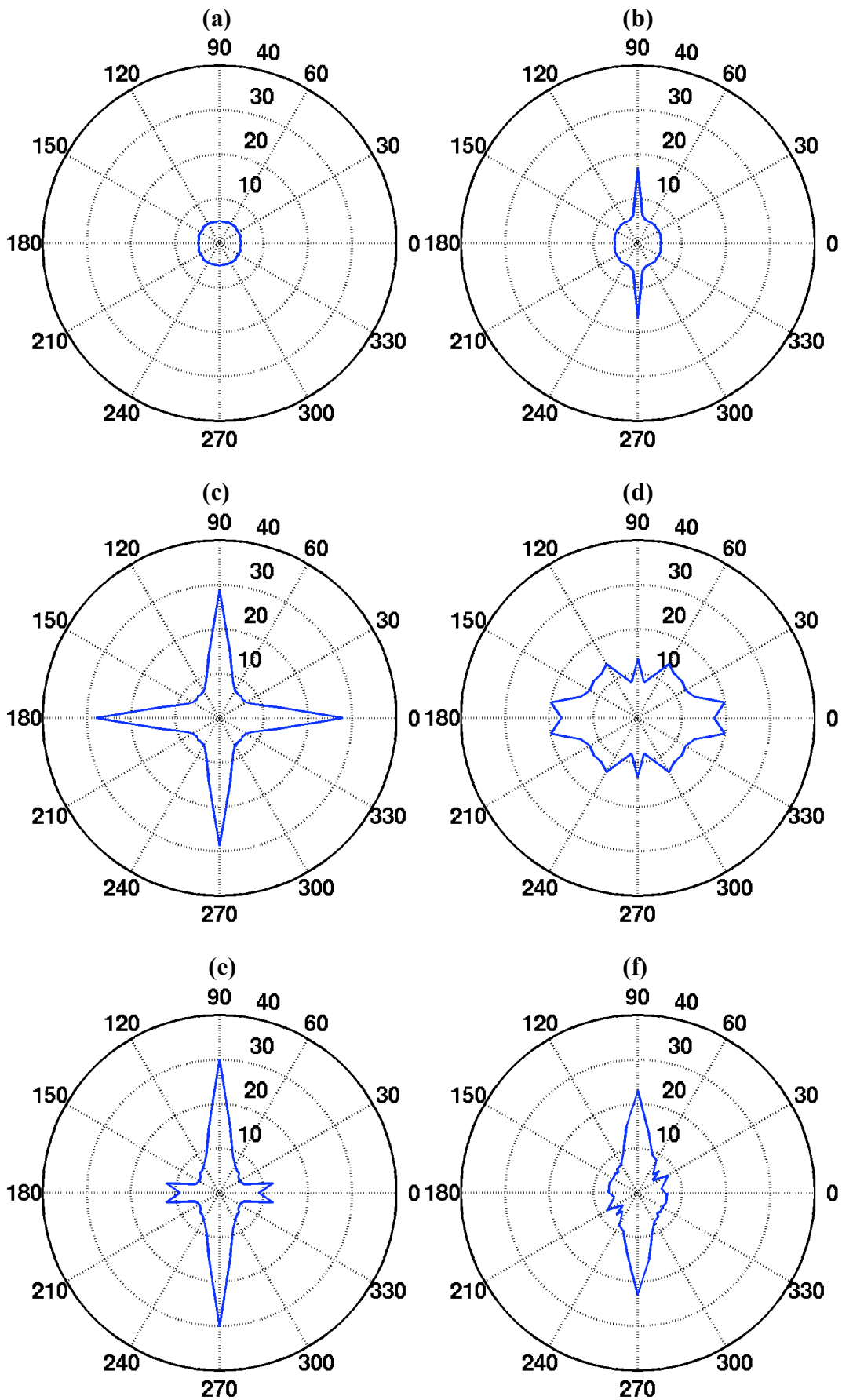


Figure 4: Azimuthal scattering index for 3-layer models (a) NoFrac; (b) X30; (c) X30 \perp Y30; (d) X30 \perp Y30Z4 \times ; (e) X30 \perp Y42; (f) X30 \angle 45 .

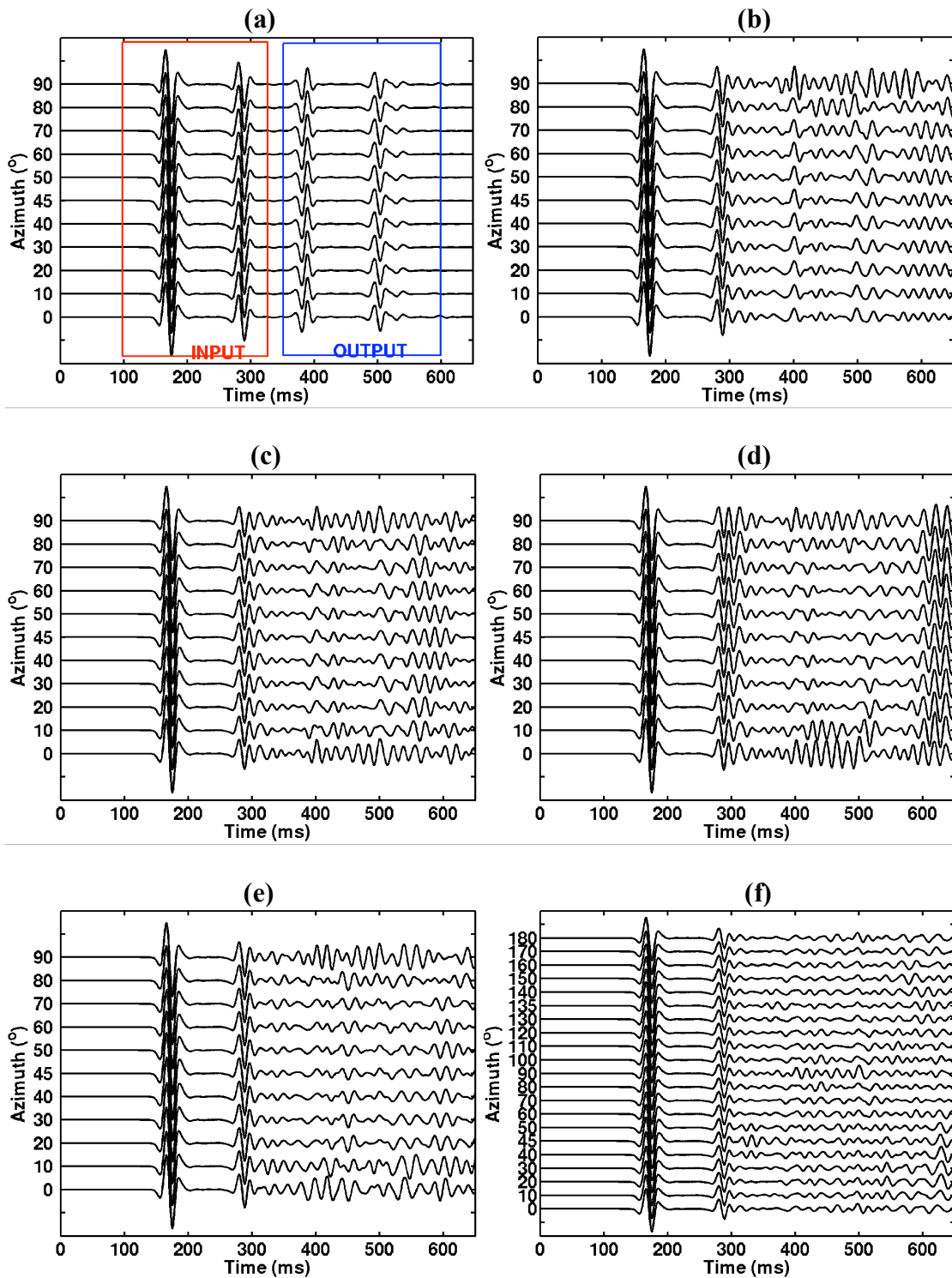


Figure 5: Azimuthal stacked traces for 5-layer models. (a) no fractures; (b) single fracture set with strike of 90 degrees (X_{35}); (c) two sets of orthogonal fractures with the same fracture compliance and spacing ($X_{35} \perp Y_{35}$); (d) same as (b) except compliance for fracture set aligned at 0 degrees is 4 times large than that at 90 degrees ($X_{35} \perp Y_{35}Z_{4\times}$); (e) two sets of orthogonal fractures with different spacing ($X_{35} \perp Y_{50}$); (f) two sets of non-orthogonal fractures at 45 degrees, 0 to 180 degrees azimuth.

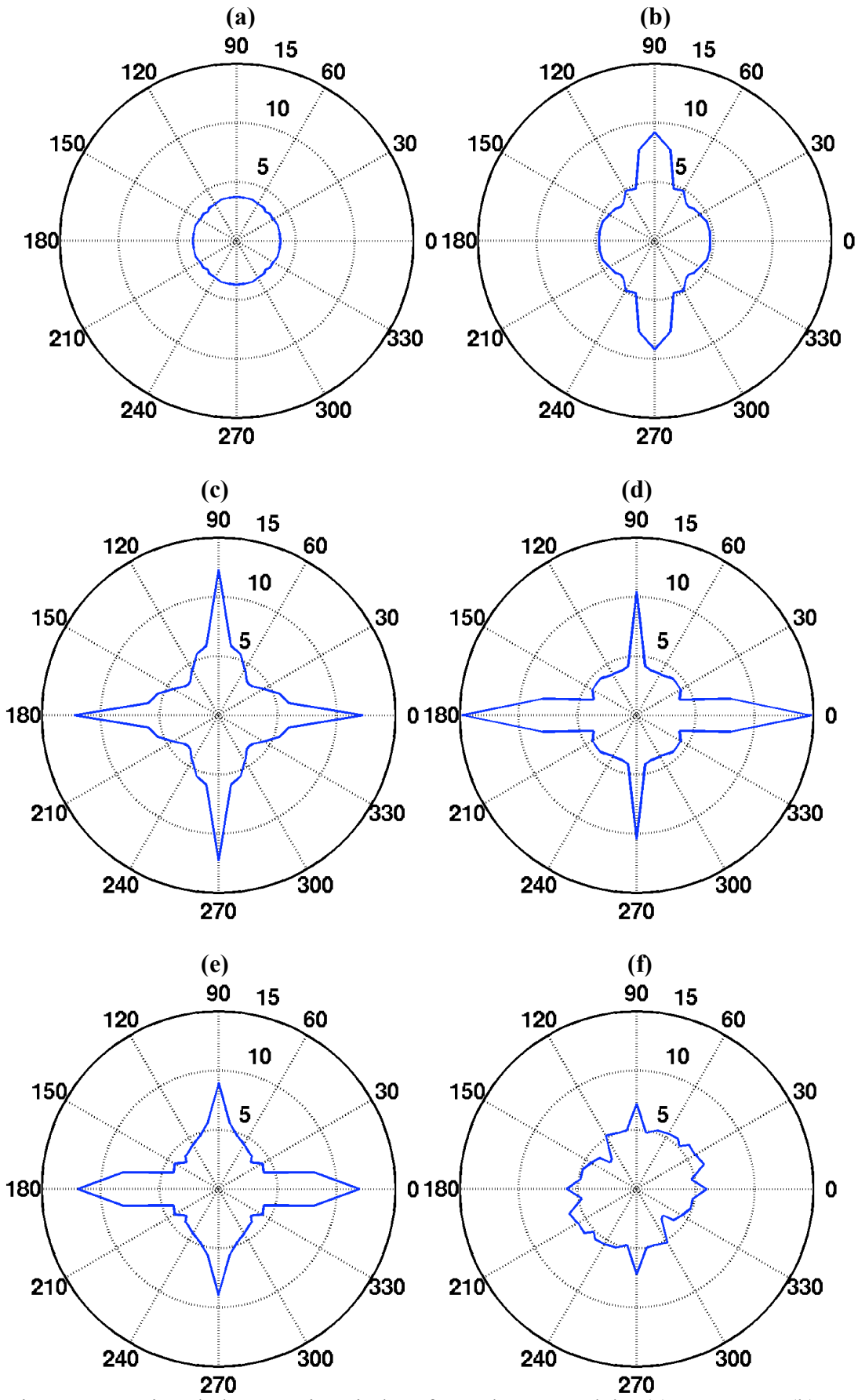


Figure 6: Azimuthal scattering index for 5-layer models (a) NoFrac; (b) X35; (c) X35 \perp Y35; (d) X35 \perp Y35Z4 \times ; (e) X35 \perp Y50; (f) X35 \angle 45.